PERGAMON

International Journal of Multiphase Flow 27 (2001) 459–475

International Journal of Multiphase Flow

www.elsevier.com/locate/ijmulflow

Intelligent identification system of flow regime of oil–gas–water multiphase flow

Haojiang Wu*, Fangde Zhou, Yuyuan Wu

State Key Laboratory of Multiphase Flow in Power Engineering, Xi'an Jiaotong University, 26 Xianning Road, Xi'an, 710049, People's Republic of China

Received 9 August 1999; received in revised form 10 March 2000

Abstract

Instantaneous differential pressure signals of oil–gas–water multiphase flow in a horizontal pipe are measured with a piezo-resistance differential pressure transducer with fast response. The signals are denoised by using wavelet theory and then the characteristic vectors of various flow regimes are obtained from the denoised differential pressure signals with fractal theory. The characteristic vectors of known flow regimes are fed into a neural network for training and later on weight coefficients of neural network are obtained through training. Then, the characteristic vector of some kind of unknown flow regime of oil–gas–water multiphase flow is fed into the neural network and the neural network can automatically send out the information in respect to the classification of flow regime, thus the intelligent identification of flow regime of oil–gas–water multiphase flow is realized. Practice shows that this new method for identifying flow regimes of multiphase flow and the system constructed with the method has the merits of high accuracy, fast response and automatic identification without artificial intervention etc. It will have promising application prospect.

Keywords: Wavelet; Fractal; Multiphase flow; Flow regime; Neural network; Pattern recognition

1. Introduction

Due to the shortage of oil resources in land, the focus of exploitation of oil and natural gas has been transferred from land to sea. There are very rich resources, such as oil and gas in the sea (for e.g., North Sea in the UK). Now more and more oil fields in the sea have been put

* Corresponding author.

0301-9322/01/$ - see front matter
PII: S0301-9322(00)00022-7

into production. As the construction of oil field on the sea is complex and expensive, it is very important to select economic and reliable method for transportation in order to save the cost of transportation. It is reported that the scheme of mixing transportation of oil and natural gas can save about 10–40% of investment on the sea. However, the design of system of mixing transportation and the selection of relevant devices are very closely correlated to the flow regime of oil–gas–water multiphase flow in the pipe. During the process of oil–gas transportation, a set of automatic devices for identifying the flow regime in the pipe are needed to monitor the flow regime and thus make the fluid flow in most effective way for transportation. The whole automatic device consists of transducers, data acquisition unit, data analysis unit and performer, thus the transportation of oil–gas is controlled without the interference of man.

Flow pattern information in gas liquid flows is usually obtained by visual observation. The designation of flow pattern has not yet been accurately standardized and depends largely upon individual interpretation of visual observations, therefore, a variety of classifications exist.

The major difficulty in visual observation, even using high speed photography, is that the picture is often confusing and difficult to interpret, especially when dealing with high velocity flows. In addition, there are systems which are opaque where flow visualization is impossible. Although considerable experimental work has been performed studying two phase gas liquid flows, not very much was done in the development of an objective device for the flow pattern classification Jones and Delhaye (1976) reviewed and summarized a variety of measuring techniques used in two phase flow of which only few are used directly for flow pattern-characterization. Hsu et al. (1963) utilized a hot wire anemometry technique for measuring void distribution for vertical flow and used the signal output also for flow pattern characterization. Jones and Zuber (1975) developed an X-ray void measurement system for obtaining statistical measurements in vertical air water flow in a rectangular channel. The probability density function of the void fraction fluctuations was used as a quantitative flow pattern discriminator for bubbly, slug and annular flow. Govier et al. (1957), Chaudhry et al. (1965) and Isbin et al. (1959) tried to relate the flow pattern to the pressure gradient variation. Their results, however, are not systematic. Furthermore, it needs mapping of the pressure gradient with flow conditions, namely the flow pattern can not be detected at one flow condition. Hubbard and Dukler (1966) suggested a method by which the flow pattern can be determined from the spectral distribution of the wall pressure fluctuations. They distinguished, however, only between separated, intermittent and distributed flows.

While all these studies have contributed to the understanding of flow regime classification, these traditional identification methods of flow regime have the shortcomings such as subjectivity and high requirements of complex measuring systems. Mi et al. (1997) recently developed a multiple neural network system with input from impedance-based measurement to classify horizontal flow regime. After training the system, the tested result was in agreement with visual observation of the authors. The advantage of the method over the former is that the trained system can automatically send out the information about flow regime. However, adopting the impedance combination of two-phase mixture as the inputs of neural network has following disadvantages. Firstly, it only suits the cases of two-phase flow, especially in which the difference of conductivity and dielectric coefficient between gas and liquid phase is rather high. Secondly, the measurement results are easyily affected by the temperature variation, the

shape and structure of the electrode and the variation of liquid phase's dielectric coefficient resulting from the impurity. Moreover, the pipe should be made of non-conducting material to ensure the pipe be electrically insulated. In order to implement automatic identification of flow regime of multiphase flow on line, the technology of artificial neural network (ANN) is adopted in this paper. At first, ANN finds out the correlation between the training samples and the expected outputs, then according to the obtained correlation, ANN computes the outputs corresponding to test samples. Because ANN can process high non-linear data with good stability and low sensitivity to noises, it has been widely used in many fields. In this paper, instantaneous differential pressure signals of multiphase flow are measured with a piezo-resistance differential pressure transducer, then the signals of the transducer are acquired through computer and processed through wavelet theory, fractal theory and ANN technology, thus an intelligent identification system of flow regime is realized.

2. Experimental apparatus

2.1. Flow loop

In this paper, mineral oil, air and water are used to simulate the horizontal oil–gas–water multiphase flow, composed of crude oil, natural gas and water in situ.

As shown in Fig. 1, water is supplied from water tank (2) and flows through a calibrated orifice flow-meter (9) into an oil–water mixer (11). Oil is supplied from oil tank (1) and also flows through a calibrated orifice flow-meter (8) into the oil–water mixer (11). Then the oil–water mixture flows into an oil–gas–water mixer (12). Air is supplied from compressor (3), flows through air pressure buffer (5) and calibrated orifice flow-meter (10) into the oil–gas–water mixer (12) and mixes with oil–water mixture. The oil–gas–water mixture then flows through test section (13) into a gas–liquid separator (14) where air is separated to the atmosphere and the oil–water mixture flows into an oil–water separator (4). The separated oil and water flow back to oil tank and water tank, respectively, for cycling utilization.

2.2. Test section

As shown in Fig. 2, the test section is made up of plexi-glass tube with inner diameter D of 40 mm. The inlet length of test section is 3.25 m ($L/D = 81.25$). The length of test section is 2 m ($L/D = 50$). The outlet length of test section is 3 m ($L/D = 75$). There are two pressure taps at the bottom of the pipe. Through tubing, a piezo-resistance differential pressure transducer is linked with the two pressure taps and used to measure pressure drop of the oil–gas–water multiphase flow between the two taps. The interval between the two taps is 205 mm.

During measurement, the medium in the tubing between taps must be the same one, either water or oil. However, because of the random phase distribution and the flow complexity, the fluctuation of the pressure drop is so large that fluid in the main pipe easily rushes into the tubing and a larger measurement error occurs. In the experiment the tubing is filled with water. At the same time, in order to prevent gas from rushing into tubing, a gas–liquid separating

box, which is filled with water, is arranged between the tube and the tap. The separating box ensures single phase liquid in the tubing and effectively reduces the measuring error.

3. Structure of the flow regime identification system

As shown in Fig. 3, the system of flow regime identification is composed of differential pressure measuring unit, data acquisition unit and data processing unit. Differential pressure measuring unit and data acquisition unit constitute the hardware part of the system, while data processing unit constitutes the software part of the system.

4. Hardware part

Differential pressure measuring unit consists of a constant current source and a piezo-resistance differential pressure transducer mentioned above.

Data acquisition unit consists of a computer and PCL-818HG data acquisition card (product of Advan Tech, Taiwan). It can do on-line acquisition and storage of the output of

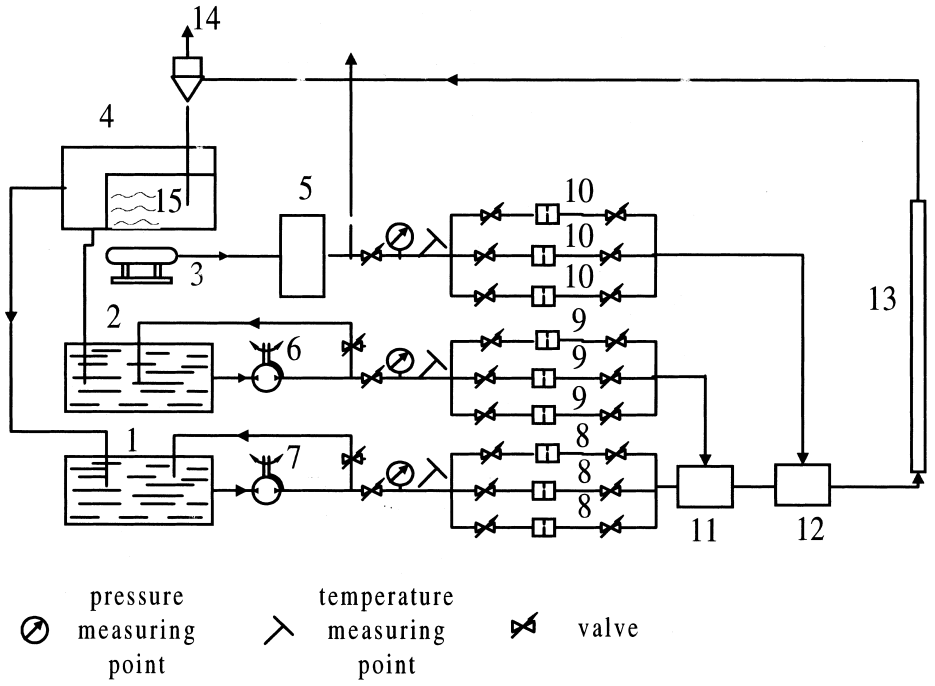

Fig. 1. Sketch of flow loop of horizontal oil–gas–water multiphase flow. 1. oil tank; 2. water tank; 3. air compressor; 4. oil-water seperator; 5. air pressure buffer; 6. water pump; 7. oil pump; 8. orifice flow meter of oil loop; 9. orifice flow meter of water loop; 10. orifice flow meter of gas loop; 11. oil-water mixer; 12. oil-water-gas mixer; 13. test section; 14. gas-liquid separator; 15. corrugated plate.

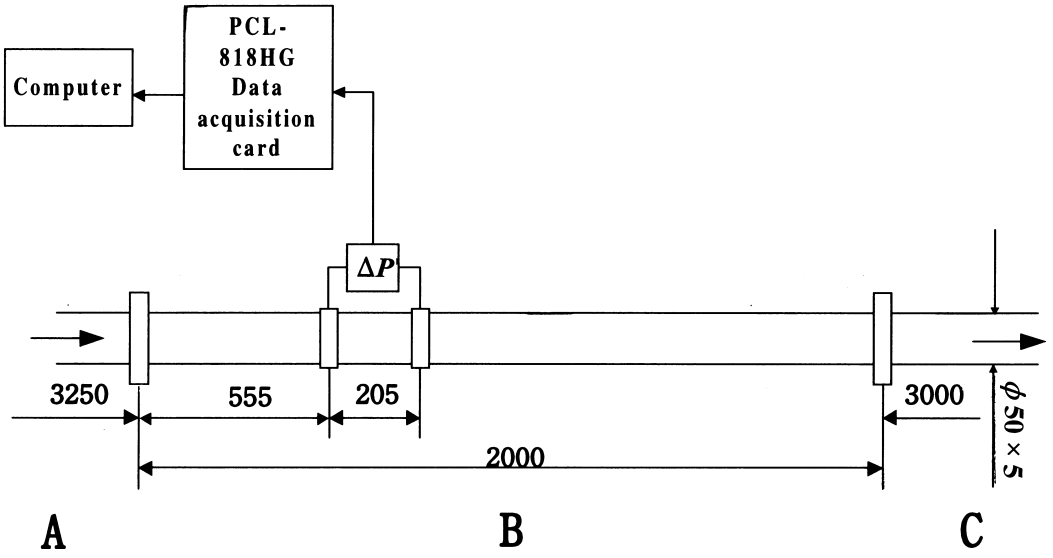

Fig. 2. Sketch of test section. A: inlet section; B: test section; C: outlet section. ΔP: piezo-resistance differential pressure transducer.

the system of differential pressure measuring. The signals are conditioned through 8115 card, converted into digital quantity through PCL-818HG card and then sent into computer. The PCL-818HG card is a high gain, high performance multi-function data acquisition card for computer. Its programmable-gain instrument amplifier (×0.5, 1, 5, 10, 50, 100, 500 or 1000)

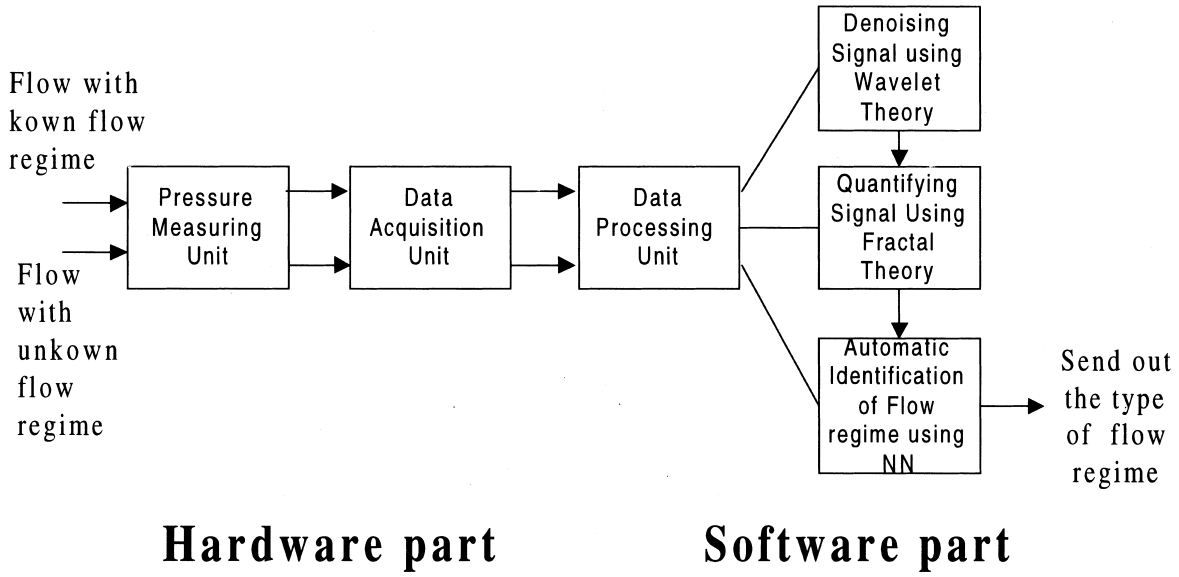

Fig. 3. Sketch of the structure of the intelligent identification system.

lets you acquire very low level input signals without external signal conditioning. An on-board 1 K word FIFO (First Input and First Output) buffer provides high-speed data transfer and perfect performance under Windows. Automatic channel scanning circuit and on-board SRAM let you perform multiple-channel A/D conversion with DMA and individual gains for each channel.

5. Software part (data processing unit)

Software unit (data processing unit) is composed of denoising, quantification of the characteristics of signals and identification with neural network. It denoises the measured differential pressure signals, then through computer implements intelligent identification which needs to quantify the characteristics of different flow regimes. Thus the characteristic vectors can be fed into neural network and the sort of flow regime are sent out as output.

5.1. Denoising the signal using wavelet theory

In order to identify flow regime of oil–gas–water multiphase flow, differential pressures of multiphase flow are measured with a piezo-resistance differential pressure transducer in this paper. However, there are always some random noises in the measured signals because of pipe vibration etc. Moreover, as the signals are input into computer after A/D conversion, the analog quantity is converted into digital quantity with limited word length, there are some errors between the ideal output and real output of the acquisition system. We refer to this error as quantization error, i.e., quantization noise. In order to identify the flow regime correctly, noises in the measured signals need to be eliminated.

5.1.1. Main idea of denoising algorithm of wavelet

The main idea of denoising signal by using wavelet theory is to discard the noise component based on the differences between the wavelet spectrum of noise and true signal at different scales (Mallat and Hang, 1992), then reconstruct the signal (without noise) using the algorithm of wavelet transform reconstruction. After the wavelet transformation, the wavelet spectrum of noise will fade at large scale while that of true signal is still very clear at large scale. Therefore, the maximum modular values of noise can be distinguished from that of true signal through the observation of evolution of the maximum modular value of true signal and noise with the variance of scales. If the amplitude of wavelet modular maximum value increases sharply with the decrease of scale, it means that the corresponding singularity has negative Lipschitz index and these maximum modular values are mainly caused by noise and should be eliminated. Thus, the maximum modular values remaing at large scales mainly belong to the true signal. Thus, we can trace the maximum modular value of the signal at different scales from large to small and find out which belong to the true signal, then reconstruct the differential pressure signal of different flow regimes. Compared to traditional denoising methods, which need to artificially determine the frequency band of noise, the method of wavelet does not need any prior knowledge of the signal and can better preserve the information of primary signals.

5.1.2. Basic steps of denoising algorithm of wavelet

1. Discrete diadic wavelet transform is performed for the discrete signal with noises. Sigularity points are searched from the pre-selected maximum scale $j = 4$.
2. The threshold $T_0 = C \cdot M/J$ is computed. M is the maximum amplitude at the maximum scale J, C is a constant.
3. Wavelet transforms at the points line $|W_{2^J}f(x)| < T_0$ at scale $j = J$ are assigned zero.
4. If $|W_{2^J}f(x)| > T_0$, then the Lipschitz exponent of corresponding point x is calculated based on the following equation

$$a = \log_2 \left| \frac{W_{2^{j+1}}f(x)}{W_{2^J}f(x)} \right|$$

   in which j is assigned 4. If a is less than 0 at some point of x, a is assigned 0.
5. The wavelet transforms of scales from 1 to $J - 1$ are assigned zero.
6. Based on the wavelet transform processed by step 3, the wavelet transforms of scales from $J - 1$ to 1 are reconstructed.
7. The signal is reconstructed based on the reconstructed wavelet transforms.

5.1.3. Examples of denoising algorithm using modulus maxima of wavelet transform

5.1.3.1. Simulation of denoising using modulus maxima of wavelet transform. In order to test the denoising algorithm, denoising of simulation signal of since wave accompanial with noises is performed, as shown in Fig. 4a.

(a) Wavelet transform of the simulation signal is first performed, then modulus maxima are selected at each scale as shown in Fig. 4b. Fig. 4b shows that noises are mainly concentrated on the smallest scales of 1 and 2.
(b) Modulus maxima which can propagate to the next scale are searched and preserved, while modulus maxima which can not propagate to the next scale are removed as shown in Fig. 4c.
(c) The signal is reconstructed with alternative projecting algorithm as shown in Fig. 4d, from which we can see that noises have been removed.

5.1.3.2. Application to oil–gas–water multiphase flow. Fig. 5 illustrates the denoising procedure of differential pressure signal of intermittent flow of oil–gas–water multiphase flow.

5.2. Quantifying the characteristics of different flow regime of oil–gas–water multiphase flow using fractal theory

It is reported that multiphase flow exhibits characteristics of fractal (Hagiwara, 1988), which is expressed by fractal dimension. So fractal dimension is adopted as the characteristics of oil–gas–water multiphase flow. Fractal dimension has many types such as information dimension

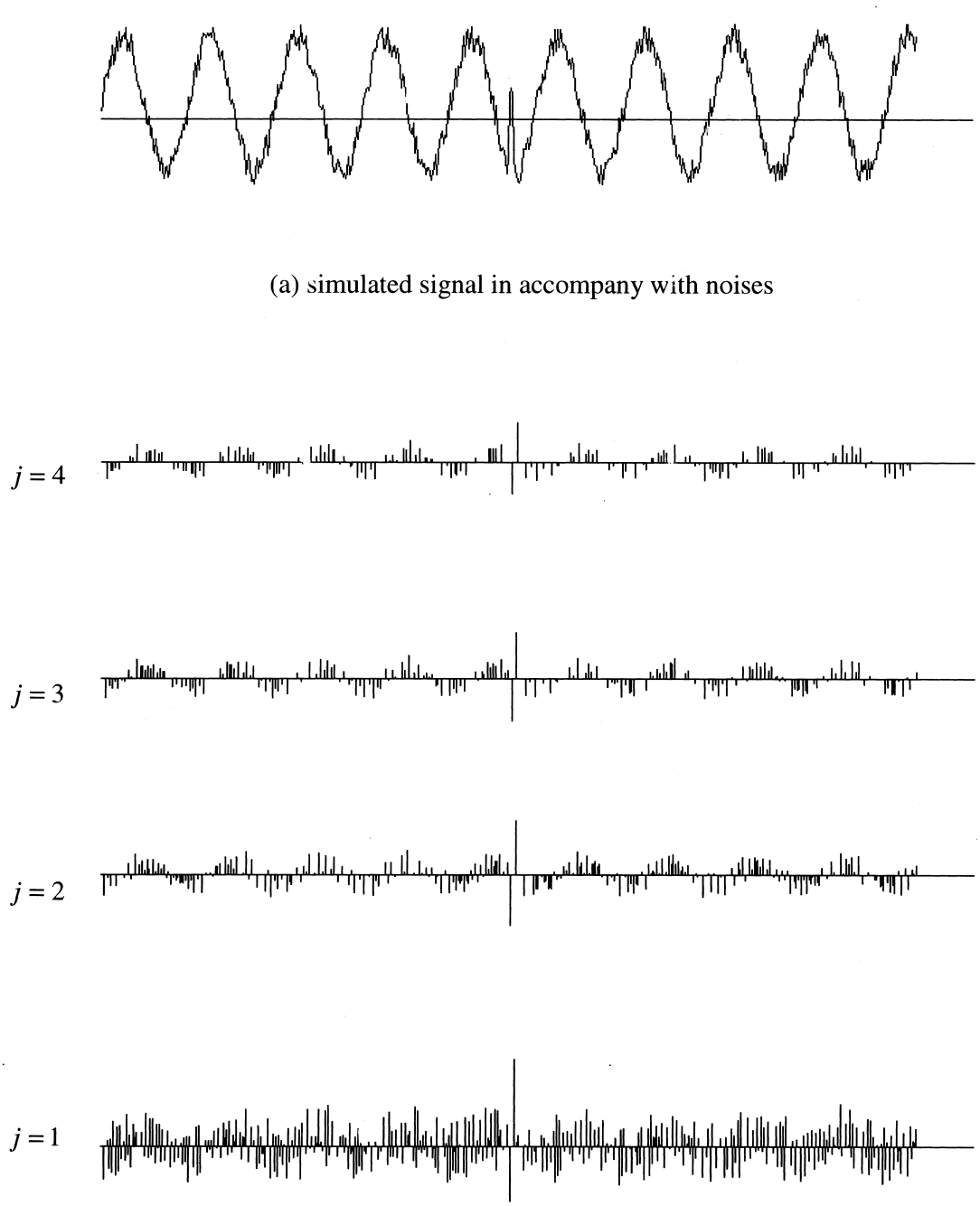

Fig. 4. Simulation of denoising using modulus maxima of wavelet transform.

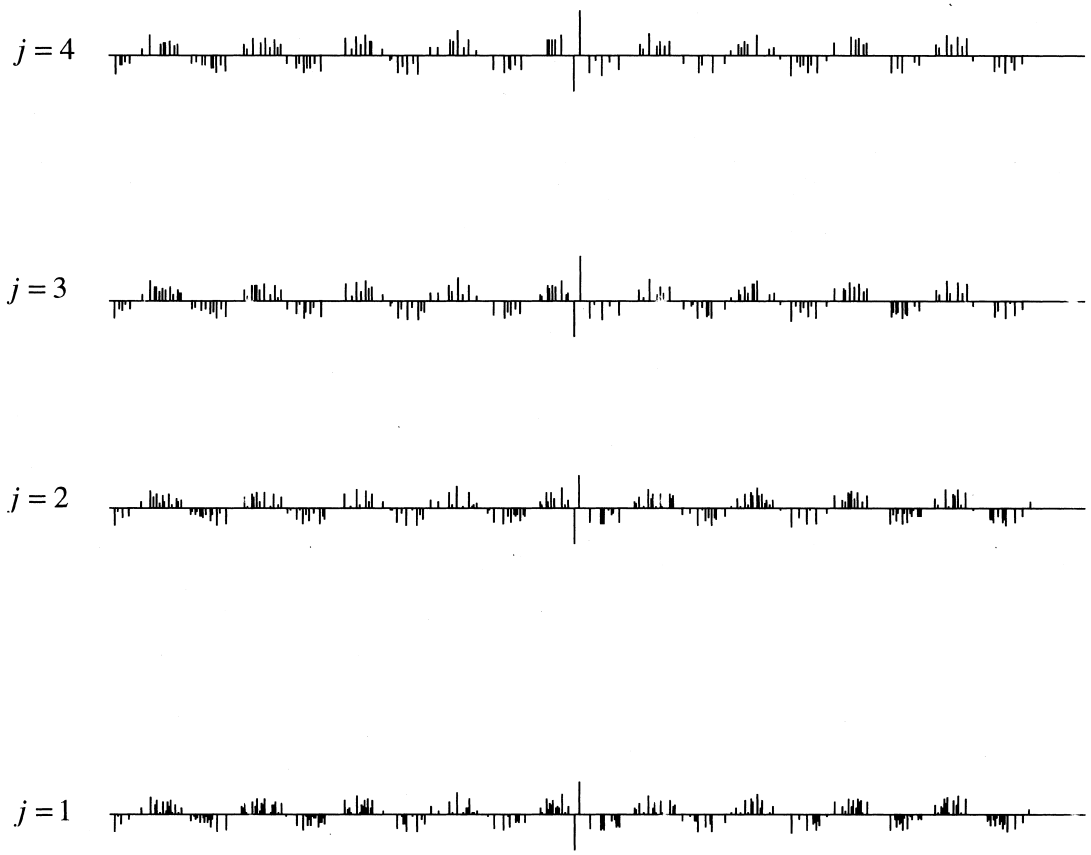

(c) modulus maxima of the simaulated signal after denoising

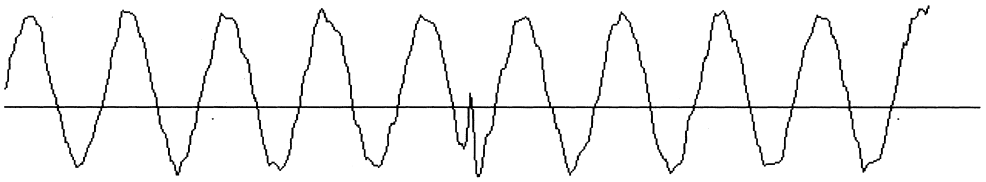

(d) the simulated signal after denoising

Fig. 4 (*continued*)

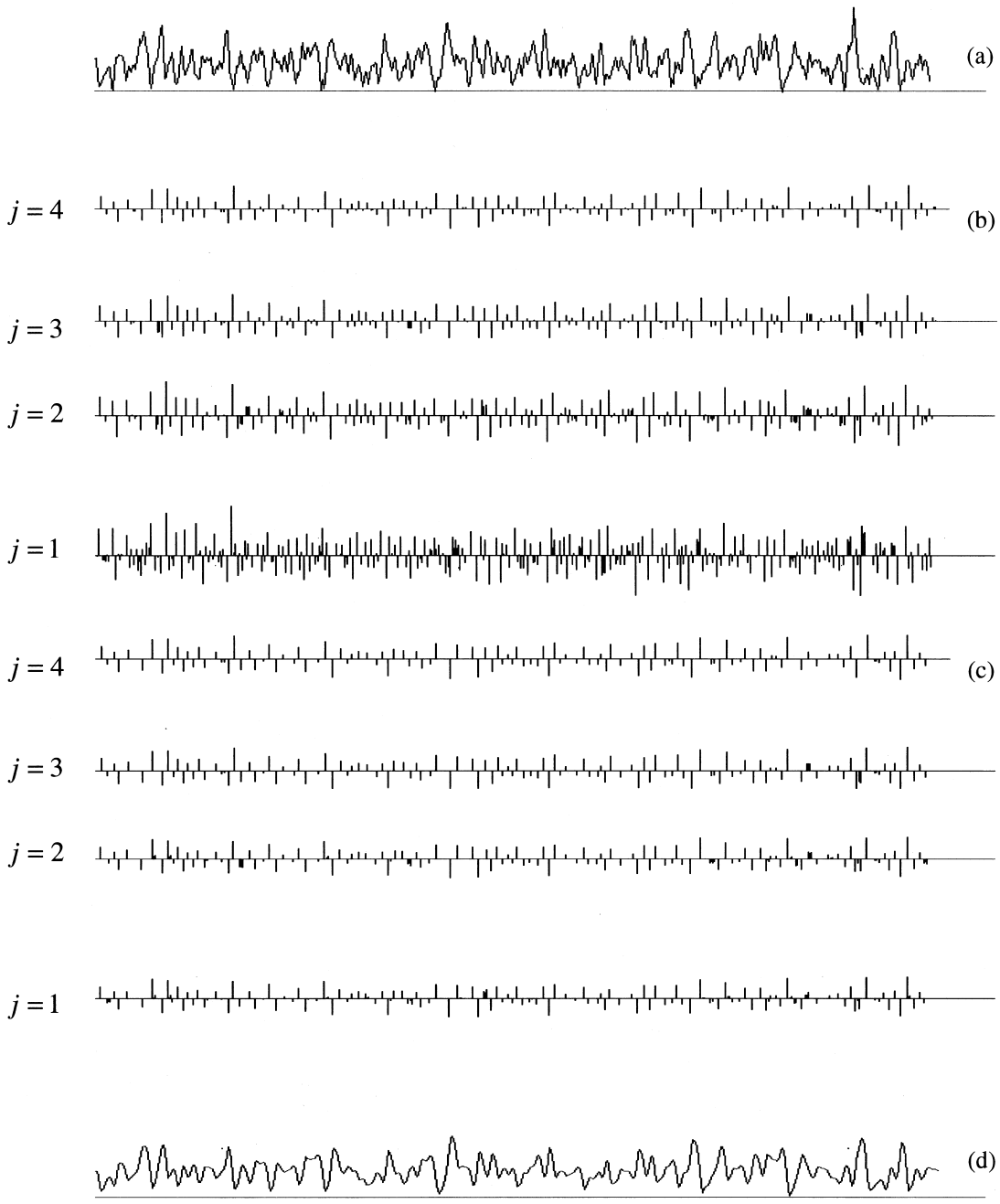

Fig. 5. Denoising procedure of differential pressure signal of horizontal annular flow of oil–gas–water multiphase flow. (a) differential pressure signal of horizontal annular flow oil-gas-water multiphase flow; (b) modulus maxima of differential pressure signal; (c) modulus maxima of denoised differential pressure signal; (d) differential pressure signal after denoising.

and correlation dimension etc. Correlation dimension (Mandelbrot, 1982) is used more often in practice.

The differential signal of oil–gas–water multiphase flow in horizontal pipe which has been sampled at equal intervals is

$$p_1, p_2, p_3, \ldots, p_i, \ldots$$

in which p_i is the differential pressure measured at time i. From this time series, vectors with dimension of m are constructed by the method of time difference.

Set $m = 5$, $y_1 = (p_1, p_2, p_3, p_4, p_5)$, then shift one step to the right, set $y_2 = (p_2, p_3, p_4, p_5, p_6)$, thus we can construct a series of vectors $y_1, y_2, \ldots, y_k$.

The absolute value of the difference between any two vectors $r_{ij} = |y_i - y_j|$ is the distance between vector y_i and y_j. Taking a certain value of ε, and compare it with all r_{ij}, the number of $r_{ij} < \varepsilon$ is $N_1(\varepsilon)$ and the number of $r_{ij} > \varepsilon$ is $N_2(\varepsilon)$. The total number of r_{ij} is

$$N = N_1(\varepsilon) + N_2(\varepsilon) = k(k-1)/2.$$

All vectors whose distance is less than the given value ε is called correlated vectors. The proportion of correlated vectors in the total number N are called correlation integral:

$$c(\varepsilon) = \frac{N_1(\varepsilon)}{N}$$

Defining correlation dimension

$$D = \frac{\ln c(\varepsilon)}{\ln \varepsilon}$$

When dealing with different flow regimes of oil–gas–water multiphase flow different pressure signals are measured with the same sampling points. Let ε be 0.1, 0.2, 0.3, 0.4, 0.5, 0.6, 0.7, 0.8, 0.9, respectively; nine correlation dimensions can be computed for each work condition of the flow.

Arrange these nine correlation dimensions as nine components of a vector. This vector is the characteristic vector of each flow regime of oil–gas–water multiphase flow at different work condition (for example the characteristic vector of the first working condition in Table 1 is (0.62, 0.38, 0.33, 0.33, 0.36, 0.43, 0.54, 0.71, 1.00)). Then, we can use characteristic vectors of different working conditions as the input vectors of neural network mentioned later in this paper.

5.3. Improving BP neural network with nonlinear least squares method

Nowadays the most popular neural network used in the field of model identification is BP neural network (Jiao, 1995) based on the back-propagation learning algorithm. As the back-propagation learning algorithm is a kind of gradient descent algorithm and has shortcomings such as liability to run into local minimum and slow learning speed etc., we apply nonlinear least squares algorithm to improve back-propagation learning algorithm. Its advantage is its very good numerical stability and convergence speed. For very large networks the memory

Table 1
Examples of characteristic vector of horizontal oil–gas–water multiphase flow

Flow Velocity of each phase of multiphase flow			Correlation dimension D_2								
Gas (m/s)	Oil (m/s)	Water (m/s)	$\varepsilon = 0.9$	$\varepsilon = 0.8$	$\varepsilon = 0.7$	$\varepsilon = 0.6$	$\varepsilon = 0.5$	$\varepsilon = 0.4$	$\varepsilon = 0.3$	$\varepsilon = 0.2$	$\varepsilon = 0.1$
2.341	0.253	0.026	0.62	0.38	0.33	0.33	0.36	0.43	0.54	0.71	1.00
3.162	0.099	0.023	0.38	0.23	0.17	0.15	0.14	0.14	0.15	0.19	0.34
6.084	0.235	0.027	0.15	0.07	0.05	0.04	0.04	0.05	0.07	0.13	0.31
5.706	0.102	0.02	4.22	2.53	2.01	1.79	1.70	1.68	1.71	1.80	1.99
6.379	0.699	0.068	0.29	0.16	0.14	0.13	0.15	0.20	0.29	0.45	0.72
2.758	0.183	0.053	0.41	0.21	0.16	0.16	0.19	0.25	0.35	0.51	0.80
6.084	0.238	0.058	0.17	0.09	0.07	0.06	0.05	0.06	0.09	0.18	0.40
5.635	0.352	0.095	1.15	0.61	0.43	0.36	0.33	0.35	0.43	0.58	0.85
10.169	0.300	0.092	0.11	0.06	0.04	0.04	0.04	0.08	0.16	0.34	0.68
3.047	0.507	0.120	0.90	0.50	0.36	0.29	0.26	0.26	0.30	0.42	0.69
5.411	0.500	0.115	1.39	0.75	0.54	0.43	0.39	0.41	0.48	0.63	0.88
9.604	0.453	0.113	0.26	0.18	0.17	0.18	0.22	0.29	0.40	0.60	0.93
3.309	0.633	0.176	1.69	0.89	0.63	0.53	0.50	0.52	0.60	0.73	0.97
7.388	0.662	0.184	0.74	0.47	0.42	0.43	0.49	0.58	0.72	0.91	1.17
10.718	0.710	0.177	4.90	3.00	2.42	2.18	2.08	2.05	2.08	2.19	2.38
13.732	0.689	0.165	5.73	3.47	2.77	2.48	2.35	2.31	2.35	2.45	2.69
2.7833	0.066	0.026	5.24	3.05	2.36	2.05	1.90	1.83	1.82	1.85	1.93
3.150	0.128	0.052	0.81	0.53	0.47	0.47	0.53	0.62	0.76	0.93	1.16
2.972	0.196	0.087	3.66	2.25	1.82	1.65	1.58	1.57	1.60	1.68	1.86
5.333	0.190	0.086	0.22	0.14	0.13	0.15	0.20	0.29	0.42	0.63	0.96
2.030	0.277	0.115	1.24	0.78	0.67	0.66	0.69	0.77	0.88	1.03	1.24
4.965	0.284	0.117	0.25	0.15	0.12	0.12	0.14	0.20	0.31	0.49	0.81
1.857	0.395	0.189	0.68	0.44	0.40	0.42	0.46	0.54	0.65	0.81	1.02
4.572	0.396	0.175	0.58	0.34	0.26	0.24	0.24	0.28	0.36	0.52	0.77
11.007	0.428	0.176	4.04	2.48	2.01	1.81	1.74	1.73	1.77	1.87	2.07
3.892	0.684	0.305	0.95	0.53	0.42	0.39	0.41	0.46	0.56	0.73	0.99
8.195	0.696	0.288	2.20	1.23	0.94	0.83	0.80	0.84	0.93	1.07	1.30
11.600	0.714	0.301	0.89	0.50	0.39	0.36	0.36	0.40	0.49	0.65	0.94
2.300	0.227	0.158	0.32	0.23	0.22	0.25	0.30	0.37	0.49	0.68	0.96
5.502	0.237	0.165	0.45	0.25	0.20	0.19	0.18	0.20	0.27	0.43	0.73
11.317	0.229	0.156	0.43	0.23	0.18	0.17	0.17	0.21	0.30	0.48	0.81
3.903	0.381	0.278	0.58	0.34	0.29	0.28	0.31	0.37	0.48	0.66	0.96
8.883	0.410	0.276	1.72	1.02	0.81	0.74	0.73	0.78	0.88	1.05	1.33
7.234	0.563	0.348	2.53	1.45	1.13	1.01	0.99	1.02	1.09	1.21	1.42
12.764	0.539	0.376	1.54	1.03	0.91	0.90	0.94	1.02	1.15	1.34	1.64
16.507	0.103	0.027	4.16	2.56	2.09	1.90	1.83	1.81	1.86	1.95	2.11
20.818	0.116	0.025	5.49	3.32	2.65	2.36	2.23	2.18	2.20	2.30	2.50
22.037	0.203	0.057	4.90	3.04	2.48	2.25	2.15	2.13	2.18	2.30	2.53
18.881	0.340	0.093	7.16	4.22	3.29	2.85	2.65	2.55	2.53	2.60	2.76
17.430	0.503	0.122	6.43	3.83	3.01	2.64	2.46	2.39	2.39	2.47	2.63
29.446	0.055	0.022	4.38	2.71	2.21	2.01	1.94	1.94	1.99	2.12	2.36
26.577	0.099	0.054	5.58	3.36	2.68	2.38	2.24	2.20	2.23	2.31	2.50
20.870	0.173	0.078	4.88	2.99	2.41	2.16	2.06	2.03	2.07	2.17	2.39
27.948	0.059	0.044	3.41	2.15	1.80	1.68	1.65	1.68	1.76	1.89	2.13

requirements of the algorithm make it impractical for most current machines (as in the case for the quasi-Newton methods). However, as in the field of intelligent identification of flow regime, weights of the neural network is not more than 1000. At this time its advantage predominates over its disadvantages. So this method is very suitable for the intelligent identification of flow regime.

Consider a three-layer feed-forward network:

node of output layer k ($k = 1, \ldots, K$),
node of hidden layer j ($j = 1, \ldots, J$),
node of input layer i ($i = 1, \ldots, I$).

W_{kj}, W_{ji} represent the weights between output layer and hidden layer, the weights between hidden layer and input layer, respectively. Arranging all weights and thresholds in the network into a vector with dimension of n.

$$w = [w_1, w_2, \ldots, w_n]^{\mathrm{T}} \tag{1}$$

Then, the mapping relationship of the neural network can be written as

$$\hat{y}(p, w) = f(x^p, w) \tag{2}$$

where x^p is the pth training model vector, $f(\bullet)$ is a nonlinear mapping. $\hat{y}(p, w)$ is the output vector of neural network.

Given a group of train models $\{x^p, y^p\}_{p=1}^N$, where y^p is the expectation output, N is the number of training models, the purpose of training of network is to minimize the distance between the network output $\hat{y}(p, w)$ and the expectation output y^p by adjusting the weight of w.

If the objective function is selected as following

$$E(w) = \frac{1}{2}\sum_{p=1}^{N}\left[y^p - \hat{y}(p, w)\right]^{\mathrm{T}}\left[y^p - \hat{y}(p, w)\right] \tag{3}$$

then the optimal weight of w can be obtained by minimizing the above objective function.

Generally iteration equation

$$w(k+1) = w(k) + \alpha_k p_k \tag{4}$$

is adopted to minimize Eq. (3).

Where k is the iteration epoch, p_k is the searching direction computed from the estimated parameter values of the former iteration. α is a small nonegative number and should be properly selected in order to ensure convergence of iteration.

In BP learning algorithm, the searching direction is adopted as $p^k = -E(w(k))$, which leads to the shortcomings mentioned above. Therefore, nonlinear least squares method is adopted to overcome BP's shortcomings. In detail, a regular term is added to objective function (3) in order to limit the range of variation of the parameter of w

$$E_k(w) = \frac{1}{2}\sum_{p=1}^{N}\left[y^p - \hat{y}(p, w)\right]^{\mathrm{T}}\left[y^p - \hat{y}(p, w)\right] + \frac{1}{2}\left[w - \hat{w}(k)\right]^{\mathrm{T}}\left[w - \hat{w}(k)\right] \tag{5}$$

In order to solve the minimum point of modified objective function (5), write the nonlinear mapping $f(x^p, w)$ in Taylor's series of the first order at the point of $w = \hat{w}(k)$

$$f(x^p, w) \approx f\left(x^p, \hat{w}(k)\right) + \nabla f\left(x^p, \hat{w}(k)\right)\left[w - \hat{w}(k)\right] \tag{6}$$

where $\nabla f(x^p, \hat{w}(k))$ is the Jacobi matrix of $f(x^p, w)$. Let

$$Y(N) = \left[y^1, y^2, \ldots, y^N\right]^{\mathrm{T}} \quad \hat{Y}(w) = \left[\hat{y}(1, w), \hat{y}(2, w), \ldots, \hat{y}(N, w)\right]^{\mathrm{T}}$$

$$\nabla f^{\mathrm{T}}(x, w) = \left[\nabla f^{\mathrm{T}}\left(x^1, w\right), \nabla f^{\mathrm{T}}\left(x^2, w\right), \ldots, \nabla f^{T}\left(x^N, w\right)\right]^{\mathrm{T}}$$

Then the modified objective function (5) can be written as

$$E(w) = \frac{1}{2}\left[Y(N) - \hat{Y}(w)\right]^{\mathrm{T}}\left[Y(N) - \hat{Y}(w)\right] + \frac{\mu}{2}\left[w - \hat{w}(k)\right]^{\mathrm{T}}\left[w - \hat{w}(k)\right] \tag{7}$$

Writing $\hat{Y}(w)$ in Taylor's series of the first order at the point of $w = \hat{w}(k)$ and then substituting the expansion series into Eq. (7), we get

$$\nabla E_k(\hat{w}(k)) \approx \nabla f^{\mathrm{T}}\left(x, \hat{w}(k)\right)\left[Y(N) - \hat{Y}(\hat{w}(k))\right] \tag{8}$$

$$\nabla^2 E_k(w(k)) = \nabla f^{\mathrm{T}}\left(x, w(k)\right)\nabla f\left(x, w(k)\right) + \mu I \tag{9}$$

Thus, using Newton iteration equation

$$w(k+1) = w(k) + \alpha_k p_k$$

$$p_k = -\left[\nabla^2 E_k(\hat{w}(k))\right]^{-1}\nabla E_k(\hat{w}(k)) \tag{10}$$

we get the learning algorithm of improved BP neural network

$$w(k+1) = w(k) - \alpha_k\left[\mu I + \nabla f^{\mathrm{T}}\left(x, w(k)\right)\nabla f\left(x, w(k)\right)\right]^{-1}\nabla f^{\mathrm{T}}\left(x, w(k)\right)\left[Y(N) - \hat{Y}(w(k))\right] \tag{11}$$

where α_k is iteration step, searching direction is

$$p_k = -\left[\mu I + \nabla f^{\mathrm{T}}\left(x, w(k)\right)\nabla f\left(x, w(k)\right)\right]^{-1}\nabla f^{\mathrm{T}}\left(x, w(k)\right)\left[Y(N) - \hat{Y}(w(k))\right] \tag{12}$$

6. Application of the improved BP neural network to the identification of flow regime

Although the flow regimes of three phase flow are very complicated, what we care in industry is mostly about the overall property of the gas–liquid interface. Therefore, in this

paper the flow regime of oil–gas–water multiphase flow is simplified into two phase flow, that is gas phase and liquid phase (The oil phase and water phase are integrated as liquid phase). Thus, the flow regimes are classified into stratified flow, intermittent flow and annular flow similar to two-phase flow regimes.

Neural network works in three steps. First it constructs a mapping relationship between known input vectors and output vectors, then it is evaluated by some testing samples, finally it used practically.

The first step requires an expected output vector for each known input vector. This pair of vectors is called a train-pair. Commonly, many train-pairs are needed to train neural network efficiently. For a certain train-pair, the error between the calculated output vector given by neural network and the expected output vector is used to update the weights of network by the method of error back-propagation algorithm. Network repeats computing the error for each train-pair and updating the weights until the global error of all train-pairs reaches an acceptable level.

In this paper, let the expected output vector of stratified flow be (1, 0, 0), that of intermittent flow be (0, 1, 0), and that of annular flow be (0, 0, 1).

The characteristic vectors mentioned in Section 5.2 are selected as the input vectors of the neural network. The neural network has one input layer and one hidden layer. The input layer consists of nine neural cells, corresponding to the nine components of the input vectors. The hidden layer consists of five neural cells. The output layer consists of three neural cells, corresponding to the three different flow regimes of oil–gas–water multiphase flow in horizontal pipe (stratified flow, intermittent flow and annular flow).

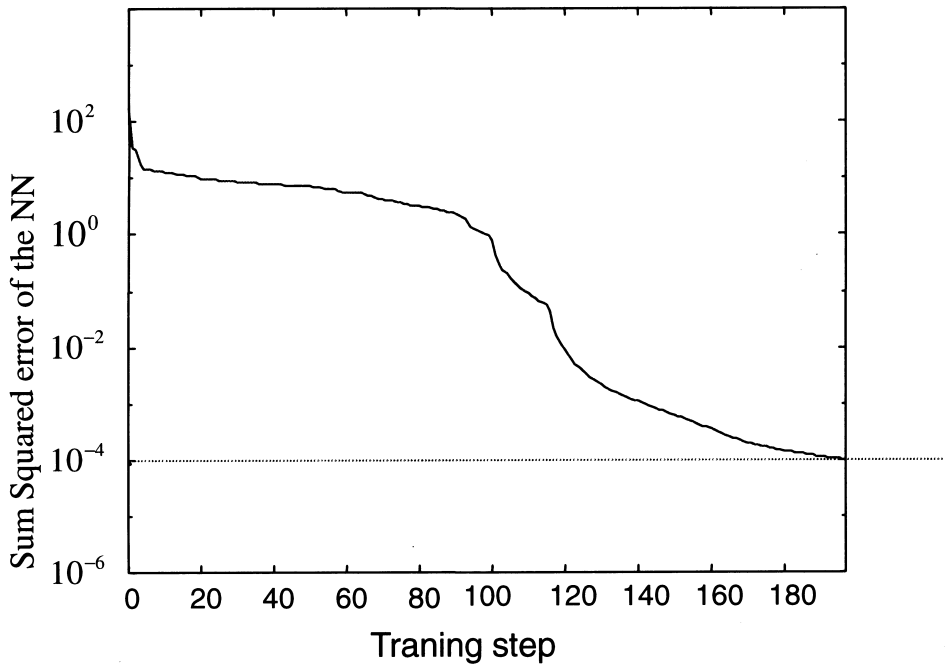

Fig. 6. The error curve of training of the improved BP NN.

Table 2
Part of test samples and identification results

Correlation dimension D_2									Identification results of NN[a]	Flow regime
$\varepsilon = 0.9$	$\varepsilon = 0.8$	$\varepsilon = 0.7$	$\varepsilon = 0.6$	$\varepsilon = 0.5$	$\varepsilon = 0.4$	$\varepsilon = 0.3$	$\varepsilon = 0.2$	$\varepsilon = 0.1$		
2.46	1.44	1.13	0.99	0.93	0.93	0.96	1.05	1.24	I	I
0.85	0.50	0.41	0.40	0.44	0.53	0.66	0.86	1.12	I	I
2.97	1.67	1.26	1.08	1.01	1.01	1.07	1.20	1.43	I	I
1.85	1.16	0.98	0.94	0.96	1.04	1.15	1.31	1.57	I	I
6.42	3.71	2.85	2.45	2.24	2.13	2.09	2.10	2.22	A	A
4.70	2.82	2.24	1.99	1.88	1.85	1.87	1.93	2.12	A	A
4.69	2.85	2.29	2.06	1.96	1.93	1.96	2.05	2.27	A	A
0.74	0.51	0.47	0.49	0.55	0.65	0.78	0.96	1.23	I	I
4.32	2.63	2.12	1.91	1.83	1.82	1.87	1.99	2.23	A	A
2.28	1.43	1.19	1.12	1.13	1.19	1.29	1.45	1.72	S	I*
4.97	3.07	2.49	2.26	2.16	2.14	2.19	2.32	2.54	A	A
5.73	3.47	2.77	2.48	2.35	2.31	2.35	2.45	2.69	I	I
6.37	3.77	2.94	2.56	2.37	2.28	2.25	2.29	2.44	A	I
4.93	3.04	2.46	2.21	2.11	2.09	2.12	2.20	2.37	I	I
3.10	1.95	1.62	1.50	1.48	1.50	1.57	1.69	1.94	I	I
0.98	0.67	0.61	0.63	0.69	0.79	0.93	1.13	1.44	I	I
1.74	1.14	1.00	0.99	1.04	1.12	1.25	1.45	1.75	I	I
0.60	0.43	0.41	0.45	0.52	0.59	0.68	0.80	0.96	I	I
1.46	0.92	0.77	0.72	0.71	0.73	0.80	0.90	1.09	I	I
2.45	1.52	1.25	1.15	1.13	1.16	1.24	1.38	1.61	S	S
2.20	1.43	1.22	1.17	1.20	1.26	1.34	1.45	1.64	S	S

[a] S denotes stratified flow, I denotes intermittent flow, A denotes annular flow, * denotes that the identification results of the NN are not in accordance with the real flow regime.

The error goal of the neural network is defined as 10^{-4}. Two hundred operating conditions of experiment are selected as training models to train the network, then 95 operating conditions are selected as test samples. The error curve of training of the improved BP neural network is shown in Fig. 6.

Identification results of the neural network after training is shown in Tables 2 and 3, from which we can find that the identification ability of the neural network is rather good.

Table 3
Identification results of improved BP neural network

	Flow regime category		
	Stratified flow	Intermittent flow	Annular flow
Number of right identification	19	46	23
Identification accuracy rating	95%	92%	92%

7. Conclusion

1. Traditional identification methods of flow regime highly depend on the subjective judgement of researchers and require complex measuring systems or instruments, therefore, the applications of the old methods in industry are limited. In addition, it sometimes needs certain parameters of the multiphase flow, which is not measurable in some important situations, for example in nuclear reactors, so the development of new methods is needed. This paper uses one piezo-resistance differential pressure transducer to measure the differential pressure of multiphase flow and through neural network intelligently identifies the flow regime without artificial intervention. This method has the merits such as high accuracy, fast and without artificial intervention etc.
2. In the past, we had to know the frequency band of the signals to denoise signals, but now we don't need the prior knowledge of signals by using maximum wavelet modular value and can preserve the information of the signal better. Therefore, the application of wavelet theory is more extensive than the traditional denoising methods.
3. Fractal dimension is used to quantify the characteristics of the differential pressure signals at different flow conditions. Results show that the method has the merits such as easy computation and easily quantifying the characteristics of the measured signals, which stand by well for the identification of the flow regime with neural network.

References

Chaudhry, A.B., Emerton, A.C. Jackson, R., 1965. Flow regimes in the concurrent upwards flow of water and air. Paper Presented at the Symp. Two-phase Flow, Exeter, 21–23.

Govier, G.W., Radford, B.A., Dunn, J.S.C., 1957. The upward vertical flow of air water mixtures. Part 1: Effect of air and water rates on flow pattern, hold-up and pressure drop. Can. J. Chem. Engng. 35, 58–70.

Hagiwara, Y., 1988. Experimental studies on chaotic behavior of liquid film flow in annular two phase flows. Physico. Chem. Hydrodanam. 10, 135–147.

Hsu, Y.Y., Simon, F.F., Graham, R.W., 1963. Application of hot wire anemometry for two phase flow measurements. In: ASME Winter Meeting, Philadelphia, PA.

Hubbard, M.G., Dukler, A.E., 1966. The characterization of flow regimes for horizontal two-phase flow. In: Saad, M.A., Moller, J.A. (Eds.), Proc. 1966 Heat Transfer and Fluid Mechanics Institute. Stanford University Press, CA, pp. 100–121.

Isbin, H.S., Moen, R.H., Wickey, R.O., Mosher, D.R., Larson, H.C., 1959. Two-phase Steam water pressure drop. Chem. Engng. Symp. Series 23, 75–84.

Jiao, Licheng, 1995. The Theory of Neural Network System. Xidian University Press, Xi'an (in chinese).

Jones, O.C., Delhaye, J.M., 1976. Transient and statistical measurement techniques for two-phase flows: a critical review. Int. J. Multiphase Flow 3, 89–116.

Jones Jr., O.C., Zuber, N., 1975. The interrelation between void fraction fluctuations and flow pattern in two-phase flow. Int. J. Multiphase Flow 2, 273–306.

Mallat, S., Hang, W.L., 1992. Singularity detection and process with wavelets. IEEE Trans. on Information Theory 38, 617–643.

Mandelbrot, B.B., 1982. The Fractal Geometry of Nature. Freeman, New York.

Mi, Y., Tsoukalas, L.H., Ishii, M., 1997. Application of multiple self-organizing neural networks: flow pattern classification. Trans. Am. Nucl. Soc. 77, 114–116.